



HAL
open science

The use of NOAA/AVHRR satellite data for monitoring and assessment of forest fires and floods

C. Domenikiotis, A. Loukas, N. R. Dalezios

► **To cite this version:**

C. Domenikiotis, A. Loukas, N. R. Dalezios. The use of NOAA/AVHRR satellite data for monitoring and assessment of forest fires and floods. *Natural Hazards and Earth System Sciences*, 2003, 3 (1/2), pp.115-128. hal-00299007

HAL Id: hal-00299007

<https://hal.science/hal-00299007>

Submitted on 18 Jun 2008

HAL is a multi-disciplinary open access archive for the deposit and dissemination of scientific research documents, whether they are published or not. The documents may come from teaching and research institutions in France or abroad, or from public or private research centers.

L'archive ouverte pluridisciplinaire **HAL**, est destinée au dépôt et à la diffusion de documents scientifiques de niveau recherche, publiés ou non, émanant des établissements d'enseignement et de recherche français ou étrangers, des laboratoires publics ou privés.

The use of NOAA/AVHRR satellite data for monitoring and assessment of forest fires and floods

C. Domenikiotis¹, A. Loukas², and N. R. Dalezios¹

¹Laboratory of Agrometeorology, Dept. of Agriculture, University of Thessaly, Fitokou Str, N. Ionia, 38446 Volos, Greece

²Department of Civil Engineering, University of Thessaly, Greece

Received: 11 February 2002 – Revised: 19 June 2002 – Accepted: 18 July 2002

Abstract. The increasing number of extreme natural phenomena, which are related to the climate variability and are mainly caused by anthropogenic factors, escalate the frequency and severity of natural disasters. Operational monitoring of natural hazards and assessment of the affected area impose quick and efficient methods based on large-scale data, readily available to the agencies. The growing number of satellite systems and their capabilities give rise to remote sensing applications to all types of natural disasters, including forest fires and floods. Remote sensing techniques can be used in all three aspects of disaster management viz: forecasting, monitoring and damage assessment. The purpose of this paper is to highlight the importance of satellite remote sensing for monitoring and near-real time assessment of the affected by forest fires and floods areas. As a tool, two satellite indices are presented, namely the Normalized Difference Vegetation Index (NDVI) and the Surface Temperature (ST), extracted by the meteorological satellite NOAA/AVHRR. In the first part of the paper, a review of utilized techniques using NDVI and ST is given. In the second part, the application of various methodologies to three case studies are presented: the forest fire of 21–24 July 1995 in Penteli Mountain near Athens and 16 September 1994 in Pelion Mountain in Thessaly region, central Greece, and finally the flood of 17–23 October 1994 in Thessaly region, central Greece. For all studies the NDVI has been utilized for hazard assessment. The method of ST has been applied to the flood event in Thessaly, for the estimation of the areal extent of the floods. As emerged from the studies, remote sensing data can be decisive for monitoring and damage assessment, caused by forest fires and floods.

1 Introduction

Natural hazards are internationally recognized as phenomena of special importance. The list of the most commonly occur-

ring natural hazards includes: asteroid, avalanche, drought, earthquake, flood, hurricane, insect infestation, landslide, volcanism, forest fire, tornado, and tsunamis. There is an increasing interest of the international community in the study of natural hazards, mainly due to the possible climate intensification by human factors. Exposure to hazard can be controlled as well as an effort can be undertaken to alleviate the effects of a hazard should one occur. There are five steps, which outline the elements of hazard monitoring and management:

- Increase preparedness and prevention, which involves activities designed to provide permanent protection from hazards such as hazard and land cover mapping and vulnerability assessment;
- Produce early warnings to minimize loss of life and damage;
- Monitor the hazard in real time;
- Assess the damage produced by the hazard;
- Provide relief, which involves assistance and/or intervention during or after hazard.

The emphasis of this study is focused on prominent environmental hazards, namely forest fires or wild fires and floods. These hazards contribute significantly to ecosystem degradation and soil erosion. Forest fires constitute a hazard that causes large damages, especially in arid and semi-arid regions. In many cases, this hazard contributes significantly to changes in the local and even global climate, soil erosion and leads to soil loss and desertification. The destruction of vegetation by forest fires can affect the land surface and the hydrologic cycle, by increasing the surface albedo, surface runoff, and decreasing the evapotranspiration (Matson et al., 1987). Moreover, the biomass burning can contribute, with gases, to the greenhouse effect and cause destruction of the ozone layer.

Forest fires occur in Mediterranean countries during the dry season and mainly affect pine forests, bushlands and

sometimes, cultivated fields. More than two thousand forest fires are annually recorded in Greece, which correspond to an average total burned area of 500 km². Although the vast majority of fires are small-scale fires, a small number of them, which is considered large-scale fires, burn extensive areas. In the USA, large-scale forest fires are considered those fires, which burn more than 4 km² (Pyne, 1984). In Greece, large-scale forest fires are considered those fires, which burn more than 1 km² (Kailidis, 1990). These large-scale forest fires represent only a 5.4% of the annual number of fires, but the burned area reaches 72% of the annually burned areas.

Other extreme meteorological phenomena are heavy storms, which result in flooding of major areas. Recently, dramatic flooding has occurred in several regions of the world for example, Mississippi River (USA, 1993), Piemonte (Italy, 1994), Rine and Meuse (Netherlands, Belgium and Germany, 1995), Biescas (Spain, 1996) and Oder (Czech Republic, Poland, and Germany, 1997). In Greece, heavy rainstorms during fall and winter months have been considered as major hazards causing flooding and subsequent significant damage to the agricultural production as well as to urban areas. The overall view of the phenomenon and mapping of the flooded areas are very important aspects in dealing with emergency situations and the quantitative estimation of the inundated area. The monitoring of the flood can minimize the loss of life and property, and the assessment of the affected areas can provide valuable information to the authorities and insurance companies. New technologies offer possibilities for assessing the hazards potential. Specifically, the possible contribution of remotely sensed data could be focused on relief and, possibly, preparedness or warning (Williams, 1994; Foot, 1994), although in many cases remote sensing can make a valuable contribution to disaster monitoring when frequency of observation is not such a prohibitive limitation.

The scope of this paper is to present monitoring and hazard assessment remote sensing techniques for case studies of forest fires and floods occurred in Greece. It deals with the forest fire of 21–24 July 1995 in Penteli Mountain near Athens, and the forest fire of 16 September 1994 in Pelion Mountain, Central Greece. The techniques applied for monitoring and mapping the affected areas is based on the estimated Normalized Difference Vegetation Index (NDVI) and surface temperature (ST) derived from the National Oceanic and Atmospheric Administration's Advanced Very High Resolution Radiometer (NOAA/AVHRR) satellite data. The third case study is the flooding event of 17–23 October 1994 in central Thessaly, Central Greece. This work attempts to accentuate the importance of the NDVI and ST in monitoring and delineation of burned and flooded areas.

The presentation of the paper has been organized as follows. Firstly, the methods used, in the international literature, to tackle the monitoring and assessment of forest fires and floods are presented with special reference to the NOAA/AVHRR data. Next, a brief presentation of the US National Oceanic and Atmospheric Administrations (NOAA) satellites and their Advanced Very High Resolution Radiometer (AVHRR) is presented, followed by the presen-

tation of the satellite indices and the techniques used in this study. Finally, the application of the NOAA/AVHRR indices in the three case studies of forest fire and flooding monitoring and assessment precedes the conclusions.

2 Remotely-sensed monitoring and assessment of forest fires and floods with remote sensing

Several types of satellite systems present a wide range of new capabilities, which can be used to assess and monitor the effect of environmental hazards or even to avoid them altogether. A major consideration for development of remote sensing for hazard assessment and disaster reduction is the extent to which operational users can rely on a continued supply of data. Meteorological satellites are used in operational programs of hazards, since they continually provide data. Besides weather forecasting, meteorological satellites have found application in several important hazard applications mainly due to the high frequency of coverage and moderate resolution. The meteorological satellite NOAA/AVHRR can contribute to operational monitoring and assessment of natural hazards (San Miguel-Ayanz et al., 2000; Dalezios, 1995).

Large-scale forest fires expand with a high propagation velocity (2.5 km/h) and usually evolve to canopy fires. In Greece, large-scale fires are closely related and influenced by the prevailing strong winds. The atmospheric environment and local meteorological conditions are therefore very significant for the fire initiation and spread, as well as in fire risk assessment (Spanos et al., 1996). Nevertheless, in complex terrain areas, where meteorological parameters are extremely variable, meteorological conditions derived from neighboring stations are usually not representative of fire conditions. In contrary, satellite sensors provide a spatially continuous set of data from which meteorological parameters can be extracted in high temporal resolution.

Remotely sensed data and techniques have been used to detect active fires and extract the extent of the burned area during the fire (Domenikiotis et al., 2002). The methods usually applied are based on the thermal signal generated by flaming and/or smouldering combustion (Matson et al., 1987; Kennedy et al., 1994; Flasse and Ceccato, 1996; Justice et al., 1996) and the daily fire growth (Chuvieco and Martin, 1994). The use of contextual algorithms (Eva and Flasse, 1996) can improve the detection of active fires.

The operational monitoring and mapping of the burned areas are very important aspects in dealing with emergency situations and the quantitative estimation of the affected area. The assessment of the damaged areas can provide valuable information to the authorities and insurance companies. The delineation of the burned area has been the subject of research, applying methodologies on images of different spatial and temporal resolution, multi-thresholding algorithms and different channel combinations. Such techniques involve the location and estimation of the aerial extent by subtracting NOAA/AVHRR NDVI images before and after the forest

Table 1. AVHRR characteristics

Channels	Wavelength (μm)		IFOV (km)
1	0.55–0.9	Visible (VIS)	1.1
2	0.725–1.0	Near Infrared (NIR)	1.1
3	3.55–3.93	Middle Infrared (MIR)	1.1
4	10.3–11.3	Thermal Infrared (TIR)	1.1
5	11.5–12.5	Thermal Infrared (TIR)	1.1

fire (Kasischke et al., 1993; Kasischke and French, 1995; Domenikiotis et al., 2002) or using maximum value composites from NDVI (Fernández et al., 1997). Algorithms have been developed for monitoring the burned areas combining NDVI (Pozo et al., 1997) or the Global Environment Monitoring Index (GEMI) (Barbosa et al., 1999) with multi-temporal brightness temperature differences. Remote sensing is a useful tool for providing information before, during and after the forest fires and floods. The contribution of remote sensing to the prediction of a sensitive area can be achieved through the estimation of parameters used to the fire risk assessment models.

Space technology with appropriate ground support systems such as disaster warning system, data collection platform, emergency terminals, etc., is being widely used to provide valuable information and services towards flood forecast, relief and management measures. In spite of limitations of cloud coverage and long periods between the satellite passages, satellites provide crucial information for precipitation forecast, flood monitoring and warning, inundation mapping and damage assessment, and flood plain management (Jayaraman et al., 1997). The NOAA/AVHRR satellite data have been used for quantitative estimation of precipitation and river stages for remote areas along with ground data collection and relay stations (Rao, 1996). Multi-temporal NOAA/AVHRR data are used for dynamic flood monitoring (Zhou et al., 2000; Sheng et al., 2001). These data were used to extract information on the variation of flooding duration, extend and depth. Satellite data give information on the flooded area and duration. These data can, then, be used to estimate the flood volume and depth using detailed Digital Elevation Models (DEM) within the framework of a Geographical Information System (GIS) (San Miguel-Ayanz et al., 2000). Furthermore, satellite data were used to drive and calibrate hydrological and hydraulic models in order to assess the flood flow features (Bates et al., 1997). Application of a GIS-integrated physically based hydrologic model was used to map the flooded risk zones during the 1993 and 1995 Meuse River and 1997 Oder River flood events with relative success (San Miguel-Ayanz et al., 2000). In these applications, the satellite data were used to assess the land cover, which is a major input to the hydrologic model, and to map the flooded area for model validation.

The mapping and the damage assessment of flood-affected areas is one of the most successful applications of satellite

remote sensing in flood management. Because of the clear difference in the spectral signatures, it is quite possible to map areas under standing water, areas from where the flood water had receded, submerged standing crop areas, etc. Successful applications of NOAA/AVHRR data for flooded area mapping and damage assessment have been reported in the international literature (Zhou et al., 2000; Sheng et al., 2001).

Besides the need for monitoring during a flood event and performing post-flooding damage assessment, the flood prevention and the management of flood plain management is a major issue. In this sense, multi-seasonal NOAA/AVHRR mosaicked images of vegetation indices have been used to identify and classify vegetation dynamics in flooded and neighboring non-flooded areas, and thus delineate the flood plain in the Yellow River basin (Hasegawa et al., 1998) and Lake Chad basin (Birkett, 2000). In another application multi-temporal NDVI from Landsat Thematic Mapper data along with other satellite indices were used to model the floodplain inundation area within an integrated GIS and remote sensing platform (Townsend and Walsh, 1998). The potential inundation surfaces were derived from regression models that related US Federal Emergency Management Agency (FEMA) flood elevations to river position and location.

3 The National Oceanic and Atmospheric Administration (NOAA) meteorological satellite

The ground resolution of the remotely sensed data ranges from 1m to more than 1 km. The choice of the appropriate resolution depends on the information desired. High-resolution images provide more information of the study area, but result into a large amount of data. On the other hand, meteorological satellites provide low resolution data, but higher temporal resolution, appropriate for monitoring and operational requirements in forest fires and floods.

An extensive tool used for environmental monitoring through remote sensing is represented by the Advanced Very High Resolution Radiometer (AVHRR) data from the US National Oceanic and Atmospheric Administration (NOAA) satellites. The NOAA satellites are the most widely used polar-orbiting meteorological satellites of the Advanced Television Infrared Observation Satellite (TIROS-N) series, circulating the Earth in an almost north-south orbit, passing close to both poles. The NOAA satellite orbits ensure

that data for many regions of the Earth are no more than six hours old, so appropriate for near real time hazard forecasting, monitoring and damage assessment.

The NOAA satellite series bear on board a suit of instruments able to measure many parameters of the Earth's surface and atmosphere. The primary instrument, carried by the satellites, is the Advanced Very High Resolution Radiometer (AVHRR). The AVHRR is a multi-spectral scanner with medium spatial resolution. The swath is 3000×6000 km, which produces overlaps of the same area and the daily coverage of the whole earth. The AVHRR sensor characteristics are shown in Table 1. Data from all the NOAA satellites are transmitted to the ground via a broadcast called High Resolution Picture Transmission (HRPT). Two of the most prominent parameters for the study of forest fires and floods are the condition of the vegetation and the surface temperature. These parameters are not extracted directly by the brightness values, as recorded by the NOAA/AVHRR sensors. In order to convert the pixel values to useful quantities, application of mathematical functions is required. In remote sensing, the formation of indices is a common practice in order to "highlight" significant ground features. The indices are, usually, application oriented and take advantage of the ground characteristics, as they appear in the recorded image. Two of most eminent indices related to environmental studies and, especially, to forest fires and floods are the Normalized Difference Vegetation Index (NDVI) and Surface Temperature (ST).

3.1 The Normalized Difference Vegetation Index (NDVI)

The spectral reflectance characteristics of the land cover indicate a degree of separation between the feature types. The measure of the spectral response permits the assessment of type of the feature as well its condition. Specifically, chlorophyll absorbs the radiation at 0.62 to $0.7 \mu\text{m}$ and reflects it in near infrared 0.74 to $1.1 \mu\text{m}$. By observing directly the plants' radiometric response, it is possible to record the canopy reactions to environmental stresses and constraints directly and in real time. Thus, a mathematical function of the visible and infrared parts of the electromagnetic spectrum can be an indicator of the presence and condition of the vegetation. This leads us to the concept of Normalized Difference Vegetation Index (NDVI), which is an indication of the amount of green vegetation.

The NDVI is obtained by combining the Channels 1 and 2, visible and near infrared, respectively. The index is given by the equation

$$\text{NDVI} = \frac{Ch_2 - Ch_1}{Ch_2 + Ch_1}, \quad (1)$$

where Ch_1 and Ch_2 are the radiances of the first two channels of NOAA/AVHRR.

Vegetation index changes in time are correlated with the Canopy Leaf Area Index (LAI). In Table 2, a classification of reflecting surfaces based on NDVI and pixel values in the gray scale (0–255) is presented. After a fire or flood, sig-

Table 2. Vegetation classification according to typical NDVI values

Soil type	NDVI	Pixel value (0–255 gray scale)
Dense vegetation	0.500	210
Intermediate green vegetation	0.140	118
Sparse vegetation	0.090	105
Bare soil	0.025	88
Clouds	0.002	83
Snow and ice	−0.046	70
Water surface	−0.257	16

nificant reduction in LAI of the forest or field is expected and values corresponding to complete lack of chlorophyll elements are sometimes expected. A vegetation index is, therefore, representative of plants' photosynthetic efficiency, and it is time varying due to changes in meteorological and environmental parameters. The NDVI values range from -1 to $+1$ (pixel values 0–255).

The delineation of burned and flooded areas depends on the type of burned vegetation, the soil type, the time interval after the fire or flood and the extent of the affected area (totally or partially burned). After the cease of a fire or the passage of a flood wave, significant reduction of the vegetation is expected and the values corresponding to complete lack of chlorophyll elements are an indication of the burned or flooded area. For these reasons vegetation indices are an acceptable technique for identifying vegetation changes and thus, for the assessment and mapping of the affected areas. Among other vegetation indices, the NDVI is the least affected by the topography and the difference between NDVI values gives the best indication of vegetation change (Lyon et al., 1998). Thus, the NDVI is a quick and efficient way for forest fire and flood monitoring and assessment of affected areas (Dalezios et al., 1998).

3.2 Surface Temperature (ST)

The Surface Temperature (ST) is a fundamental thermodynamic quantity in the energy exchange between the surface and the atmosphere and plays an important role in environmental studies. Continuous measurements of this parameter are likely to yield information about the suspected climate change, land-use etc. Ground measurements are not appropriate for generalized heterogeneous surfaces as the ST varies according to the type and condition of the land cover. Satellite information is the only source for the mapping and monitoring of ST at small-scale. Estimation of ST is easier over the sea surface, because the emissivity over the land surface may vary significantly due to differences in surface features, topography, vegetation composition, vegetation coverage and moisture content and the observational conditions (i.e. wavelength, pixel resolution and observation angle) (Gupta et al., 1997; Dech et al., 1998).

Table 3. Summary of split-window algorithms for the estimation of the surface temperature (T_s , T_4 , T_5 , $\sigma \varepsilon^\circ K \mathcal{K}_{\text{at}}$, $T_0 = 273.15^\circ K$, $\varepsilon = (\varepsilon_4 + \varepsilon_5)/(2)$)

Algorithms	References
$T_s = [T_4 + 3.33(T_4 - T_5)] \left[\frac{5.5 - \varepsilon_4}{4.5} \right] + 0.75T_5(\varepsilon_4 - \varepsilon_5)$	Price (1984)
$T_s = T_4 + 3.00(T_4 - T_5) + 51.57 - 52.45\varepsilon$	Olivieri et al. (1985)
$T_s = 1.274 + A \frac{T_4 + T_5}{2} + B \frac{T_4 - T_5}{2}$	Becker and Li (1990b)
where $A = 1 + 0.15616 \frac{1 - \varepsilon}{\varepsilon} - 0.482 \frac{\varepsilon_4 - \varepsilon_5}{\varepsilon^2}$, $B = 6.26 + 3.98 \frac{1 - \varepsilon}{\varepsilon} + 38.33 \frac{\varepsilon_4 - \varepsilon_5}{\varepsilon^2}$	
$T_s = 3.45 \frac{T_4 - T_0}{\varepsilon_4} - 2.45 \frac{T_5 - T_0}{\varepsilon_5} + 40 \frac{1 - \varepsilon_4}{\varepsilon_4} + T_0$	Prata and Platt (1991)
$T_s = T_4 + A(T_4 - T_5) + B$	Sobrino et al. (1991)
where $A = 0.349W + 1.320 + (1.385W - 0.204)(1 - \varepsilon_4) + (1.506W - 10.532)(\varepsilon_4 - \varepsilon_5)$ $B = (1 - \varepsilon_4) / \varepsilon_4 T_4 [-0.146W + 0.561 + (0.575W - 1.966)(\varepsilon_4 - \varepsilon_5)] + (1 - \varepsilon_5) / \varepsilon_5 T_5 [-0.095W + 0.320 + (0.597W - 1.916)(\varepsilon_4 - \varepsilon_5)]$	
$T_s = 1.0162T_4 + 2.657(T_4 - T_5) + 0.5265(\sec \theta - 1)(T_4 - T_5) - 4.58$	NESDIS (Mayet et al., 1992)
$T_s = T_4 + 1.06(T_4 - T_5) + 0.46(T_4 - T_5)^2 + 53(1 - \varepsilon_4) - 53(\varepsilon_4 - \varepsilon_5)$	Sobrino et al. (1993)
$T_s = T_4 + 1.8(T_4 - T_5) + 48(1 - \varepsilon) - 75(\varepsilon_4 - \varepsilon_5)$	Olivieri et al. (1994)
$T_s = NDVI_n * T_{sv} + (1 - NDVI_n) * T_{sg}$	Gupta et al. (1997)
where $NDVI_n = [(NDVI - NDVI_{\text{soil}}) / (NDVI_{\text{veg}} - NDVI_{\text{soil}})]$ $T_{sv} = \text{ground fully vegetated}$ $T_{sg} = \text{un covered ground}$	

For the calculation of the surface temperature the knowledge of the surface emissivity is required. Surface emissivity is a measure of the inherent efficiency of the surface in converting heat energy into radiant energy above the surface. According to Sobrino et al. (2001) this subject has not been studied extensively. The ST emissivities can be estimated by five different types of methods (Kerényi and Putsay, 2000): (a) average-variance statistical relationship of emissivity, (b) space measurements (e.g. TISI algorithms), (c) in-situ or laboratory measurements, (d) the use of NDVI data, and (e) the inverse technique. One of the main factors determining the variation of the active surface temperature is the state of the vegetation cover. It can be well characterized by the NDVI (Csizsár and Kerényi, 1995). The statistical relationship between logarithm of NDVI and the surface emissivity can be given by (Sobrino et al., 1991):

$$\varepsilon_{8-14} = 1.0094 - 0.047 * \ln(\text{NDVI}), \quad (2)$$

where, $\varepsilon_4 = \varepsilon_{8-14} - 0.03$ and $\varepsilon_5 = \varepsilon_{8-14} + 0.01$.

After the emissivity is estimated a surface temperature algorithm can be applied. Table 3 gives some of the most common algorithms for the calculation of the ST. These methods are mainly based on the combination of the infrared channels. Among them is the TISI algorithm (Becker and Li, 1990a; Becker and Li, 1990b) based on the thermal infrared radiances, and the method, which estimates the emissivity value from NDVI (Van de Gried and Owe, 1993). These two categories have been validated with in-situ measurements (Kerényi and Putsay, 2000). A process for the estimation of sea surface temperature SST is based on an algorithm utilized by the NOAA/AVHRR Receiving and processing system of

BURL (Bradford University Research Limited) (B.U.R.L., 1993). According to this algorithm scaling is set so that $10^\circ C$ equates to pixel value 50 and the increment is 0.1° per value:

$$\text{SST}(^\circ C) = 10 + \frac{p - 50}{10}, \quad (3)$$

where p is the pixel value. With this standard tool, the sea surface temperature (SST) from 1° to $30^\circ C$ is estimated.

Study over an extensively wheat growing track during different growing phenological stages (Gupta et al., 1997) and slope of the morning temperature (Csizsár and Kerényi, 1995) indicated a correlation between the ST and the NDVI. Sobrino and his associates (Sobrino et al., 2001) developed a NDVI based algorithm for the estimation of ST and showed that this method shows promising results. As the ST is strongly correlated to the land cover (as expressed by the NDVI) can play a semantic role to the operational study of forest fires and floods. The ST algorithms can contribute to the forecasting, monitoring and damage assessment of natural hazards. However, more research is required towards this application field.

4 Case studies

Two cases of the monitoring of the forest fire development and the mapping of the burned area are studied and presented in this paper. Firstly, the forest fire in the Penteli Mountain which lasted from 17 to 24 July 1995 and secondly, the forest fire in the Pelion Mountain occurred on 16 September 1994 are presented. Furthermore, the estimation of the flooded area in central Thessaly during the widespread storm event of 17–23 October 1994 using the NDVI and SST index is presented.

4.1 Forest fire of Penteli Mountain, Athens, Greece (21–24 July 1995)

The study area comprises part of the Penteli Mountain, located northeast of Athens, Greece (Fig. 1, area A). A forest fire, during 21–24 July 1995, destroyed a forested area of about 63 km^2 . The dataset used for this study is a series of daily NOAA/AVHRR images acquired before, during and after the forest fire and two Landsat TM images acquired before (13 June 1995) and after (27 July 1995) the event. The Landsat TM images were selected because their high resolution was regarded adequate for optical delineation of the burned area.

The accuracy of the estimated damaged area derived from Landsat TM (or other natural resources satellites with high spatial resolution), is expected to be higher compared to that obtained from NOAA/AVHRR. However, operational needs impose the near real-time monitoring of the forest fire and estimation of the burned area. This can be achieved only by using meteorological satellite data from NOAA/AVHRR, which has the appropriate temporal resolution and can be readily available by local receiving stations. In this case, knowledge of the agreement of NOAA/AVHRR derived areal

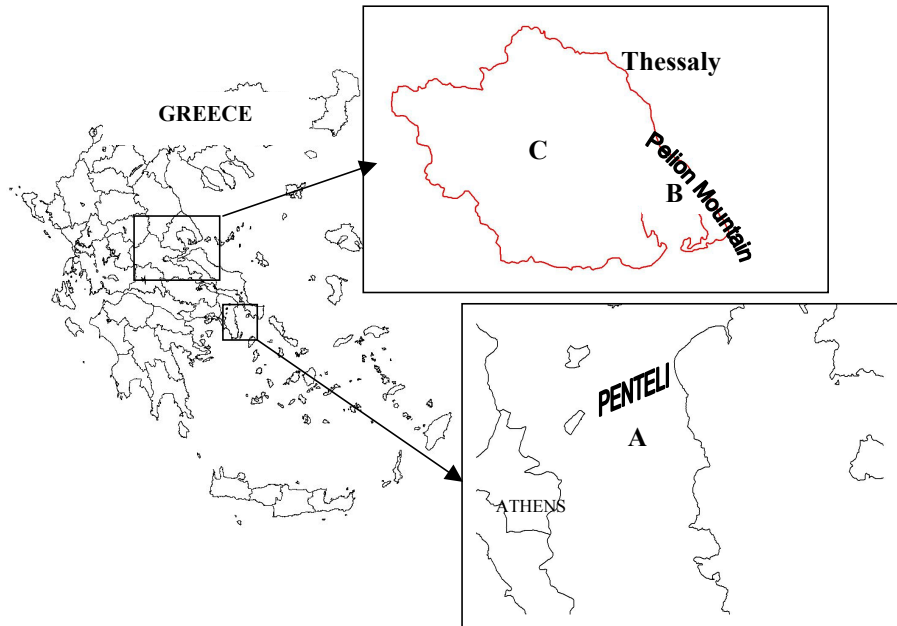


Fig. 1. The study areas for forest fires are located in (a) Penteli, Attiki and (b) mount Pelion, Greece.

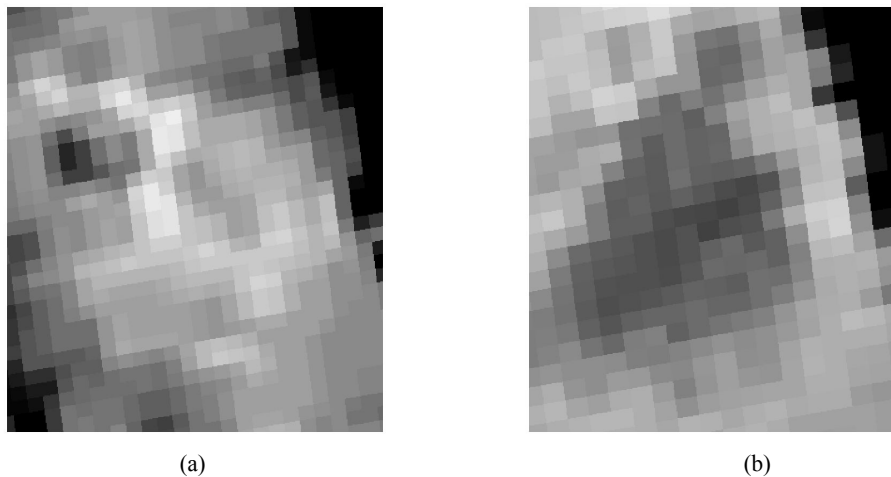


Fig. 2. NDVI images formed by NOAA/AVHRR data before (a) and after (b) the forest fire in Penteli, Greece.

extent is necessary for the initial assessment of burned areas in near-real time. So, satellite data before and after the initiation of this small-scale fire were examined.

The NDVI values were derived from the NOAA/AVHRR images. Figures 2a and 2b show the NDVI images of NOAA/AVHRR. The first image was obtained the day before the initiation of the forest fire and the second the day after the extinction of the fire. The bright areas in the first image indicate the presence of vegetation and the gray areas correspond to the suburban area of Athens and the sea. In Fig. 2b the light gray pixels indicate the burned areas.

The accuracy assessment of the NOAA/AVHRR NDVI images requires the use of a reference map defining the burned and non-burned areas. Additionally, a method for

detecting the burned areas by means of NDVI requires the use of multi-temporal images. The methodology followed involves the selection of a colour composite to assist the visual interpretation, discrimination of the burned areas and the accuracy assessment of the retrieved results.

The first step for assessing the accuracy of the method is to determine the burned areas and distinguish them from the unburned. For the study area, there are no available maps or aerial photographs, which would have indicated the burned area precisely. Thus, the accuracy of the results should be based on visual interpretation of the satellite imagery after the fire. Although, this is not the ideal way of obtaining a reference map of the burned area, due to the subjective photo-interpretation, nevertheless this method can be ap-

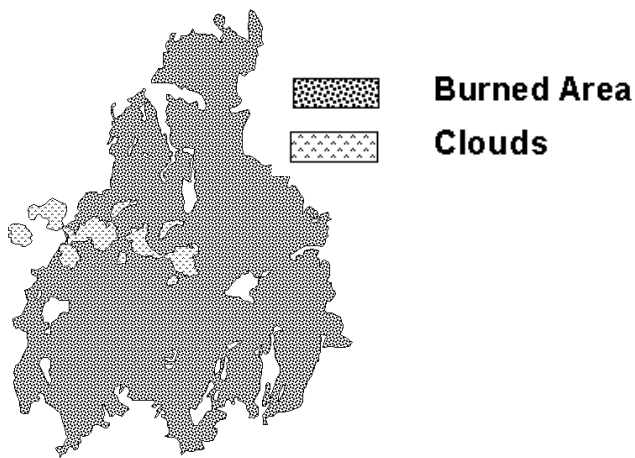


Fig. 3. The polygons delineate the burned area derived by optical interpretation and digitization of the colour composite Landsat TM image after the forest fire. The clouds were also digitized along with their shadows. This layer was used as a base map, indicating the burned area.

plied in order to obtain an indication of the accuracy of the results. Koutsias and Karteris (1998) have shown that the colour composite of TM7, TM4 and TM1 displayed in red, green and blue, respectively, allows better visual interpretation of the Landsat TM images. This false colour composite image can enhance the visual discrimination between burned land and other land use/cover categories.

The Geographic Information Systems (GIS) allow the coding, storing, analyzing and retrieving the geographic data. GIS provides a range of analytical capabilities, which are able to combine spatial and non-spatial attributes. These capabilities of synthesis allow the user to work interactively or not in order to perform the required analysis. In order to delineate the burned area, the digitization method is selected, because it allows the recognition of the areas, which are distinctly identified by the user on the colour composite image. The colour composite Landsat TM image is used to create polygon representation of the burned area. In places where the distinction is not clear, the colour composite image before the fire assisted the interpretation by direct visual comparison of the area in order to identify any possible changes. Figure 3 shows the burned area and clouds derived from the visual interpretation. The resulted area is 63.236 km^2 , which is regarded as a good approximation to the true value.

The relationship of data file values in two bands of a multi-spectral NOAA/AVHRR NDVI image can be expressed with the scatter plot. In a scatter plot, the values of one band are plotted against those of the other. If the values are equal, then the pixel values will be plotted along the diagonal axis. When both bands have normal distribution then the result is an ellipse. Any change in the brightness values between the two bands would result into a “grouping” of pixel values away from the diagonal axis.

Creating the scatter plot of the NDVI image before the forest fire against the NDVI image after the fire, the pixels

moved away from the diagonal axis can be detected. In order to distinguish the burned area from the unburned area, a threshold selection criterion is established. Figure 4a shows the scatter plot of the NDVI before and after the fire for the Landsat TM data. In this Fig. 4, the x -axis corresponds to the data after the fire and the y -axis to the data before the fire. The scatter plot indicates that there are two clusters of pixels. The area A, along the $x - y$ line, corresponds to the pixels whose values have not changed during the days. On the other hand, the area B indicates that pixels with high values, during the pre-fire period, are reduced in the after the fire image. Area B is actually the cluster of pixels, which correspond to the burned area.

Using a two-dimensional threshold these pixels can be isolated. Pixel values of NDVI images are recoded to new values. The values of the first layer below the threshold, are assigned with the value “1”, and the rest with the value “0”. As a result, two binary images are created for the Landsat TM; one for the NDVI image before the forest fire (Fig. 4b), and the second for the NDVI image after the forest fire (Fig. 4c). Each of these themes contains different information about the NDVI values. The goal of this process is to create a layer that shows only the pixels that correspond to the area B, and indicate the changes through time. The extracted map of the burned/unburned areas has to result from the combination of the extracted binary images of the two pairs of binary images for NOAA/AVHRR.

Applying the Boolean logic the attributes of the layers can be combined to provide the common area. The operator used, from Boolean algebra, is the AND. As a result, if the pixels for both maps have the attribute “1” for the burned area then the result will be a pixel with attribute “1”. The other possible combinations imply the value “0”. The final map indicates the common areas corresponding to the burned areas assigned with the value “1” and non burned areas assigned with the value “0”. This binary image shows the pixels with high values in the first NDVI image and low in the second. The layer of clouds is subtracted resulting into Fig. 4d. The same procedure is repeated for the two NDVI images derived from the NOAA/AVHRR.

The methods usually developed for mapping the burned areas are based either on the thermal signal or the use of an index or an algorithm utilizing both (thermal and index) information. When a technique is applied for operational purposes, the accuracy of the derived map needs to be known, in order to increase the credibility of the extracted results. It is thus appropriate not only to have on hand a quick and efficient method, but also to reach an acceptable degree of accuracy, which can be achieved by this method, thus indicating its usefulness as well as of the sensor from which the data are obtained.

The map of Fig. 4d was combined with the reference map (Fig. 3) to display the overlapping areas and the characteristics of the area as identified by the NOAA/AVHRR data and the result is the map of Fig. 5. The red colour indicates the correctly identified burned area, which coincides with the derived burned area from the method described above. The

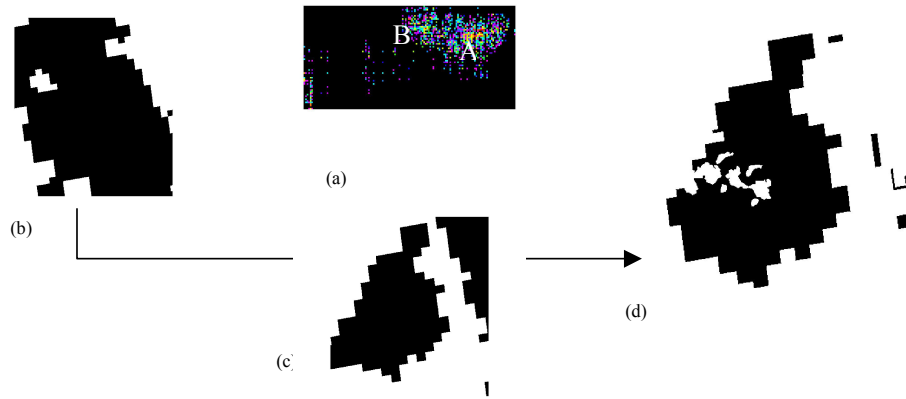


Fig. 4. (a) scatterplot of the NOAA/AVHRR NDVI image after (x -axis) and before (y -axis) the forest fire. The two binary images (b) and (c) resulted from the threshold of the two NDVI images. The image (d) corresponds to the overlay of (b) and (c) after the clouds have been removed.

Table 4. Confusion matrix comparing the reference map with the extracted burned area from NOAA/AVHRR data

	Burned area	Non-burned area	number of pixels	% agreement
Estimated burned area	49947	8139	58086	85.99%
Estimated non-burned area	18160	104605	122765	85.21%
Total	68107	112744	180851	85.46%

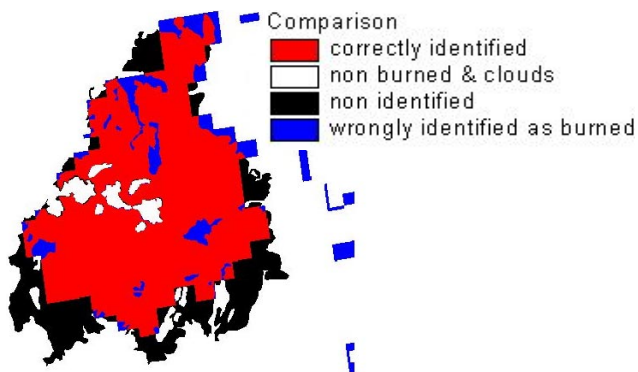


Fig. 5. Comparison between the burned area, as identified by the NDVI images, before and after the forest fire, and the reference map, for NOAA/AVHRR data sets.

black polygons correspond to burned areas, which are not identified by the method. The blue small polygons are the areas labeled as burned by the method, but they are actually not burned. The white polygons indicate the non-burned areas and areas covered by clouds. The quantitative estimation of this map is given in Table 4. Domenikiotis and his associates (Domenikiotis et al., 2002) compared the accuracy of both NOAA/AVHRR and Landsat TM data sets and showed that the overall accuracy of both sensors is similar (Table 4 and Table 5), although Landsat TM identifies more accurately details of the burned area.

The monitoring of the forest fire was achieved by us-

ing images derived from the NOAA/AVHRR data. Satellite data were examined during the large-scale fire in Penteli Mountain. The estimation of the burning areas was based on the combination of the three infrared channels 3, 4 and 5 of NOAA/AVHRR (Table 1). The process applied for this case study was based on the algorithm utilized by the NOAA/AVHRR Receiving and Processing System of BURL (Bradford University Research Limited) (B.U.R.L., 1993). According to this algorithm, an image is derived from Channels 3, 4 and 5 using Channel 4 to act as the general temperature scaled background, Channel 3 for hot spot detection and Channel 5 is used to detect clouds. A threshold value can be declared to the algorithm (e.g. 49°C), of the image processing system, and an image with hot spots, above the threshold, will be presented. The images in Figs. 6a–d are extracted based on this process. These figures show a series of images taken in the morning of 21 July 1995, the evening of the same day, 22 and 25 July 1995, respectively. The dark pixels within the rectangle show the area where the surface temperature is greater than 49°C for Figs. 6a to c. The threshold of 46°C was used for the Fig. 6d image since the temperature was dropped after the fire. The temperature images identified the burned area, in Penteli forest. The total burned area was also estimated to be 63 pixels (63 km^2).

4.2 Forest fire of Pelion Mountain, Central Greece (16 September 1994)

The forest fire was initiated in an olive field at the foothills of Pelion Mountain in central Greece (Fig. 1, area B) on 16

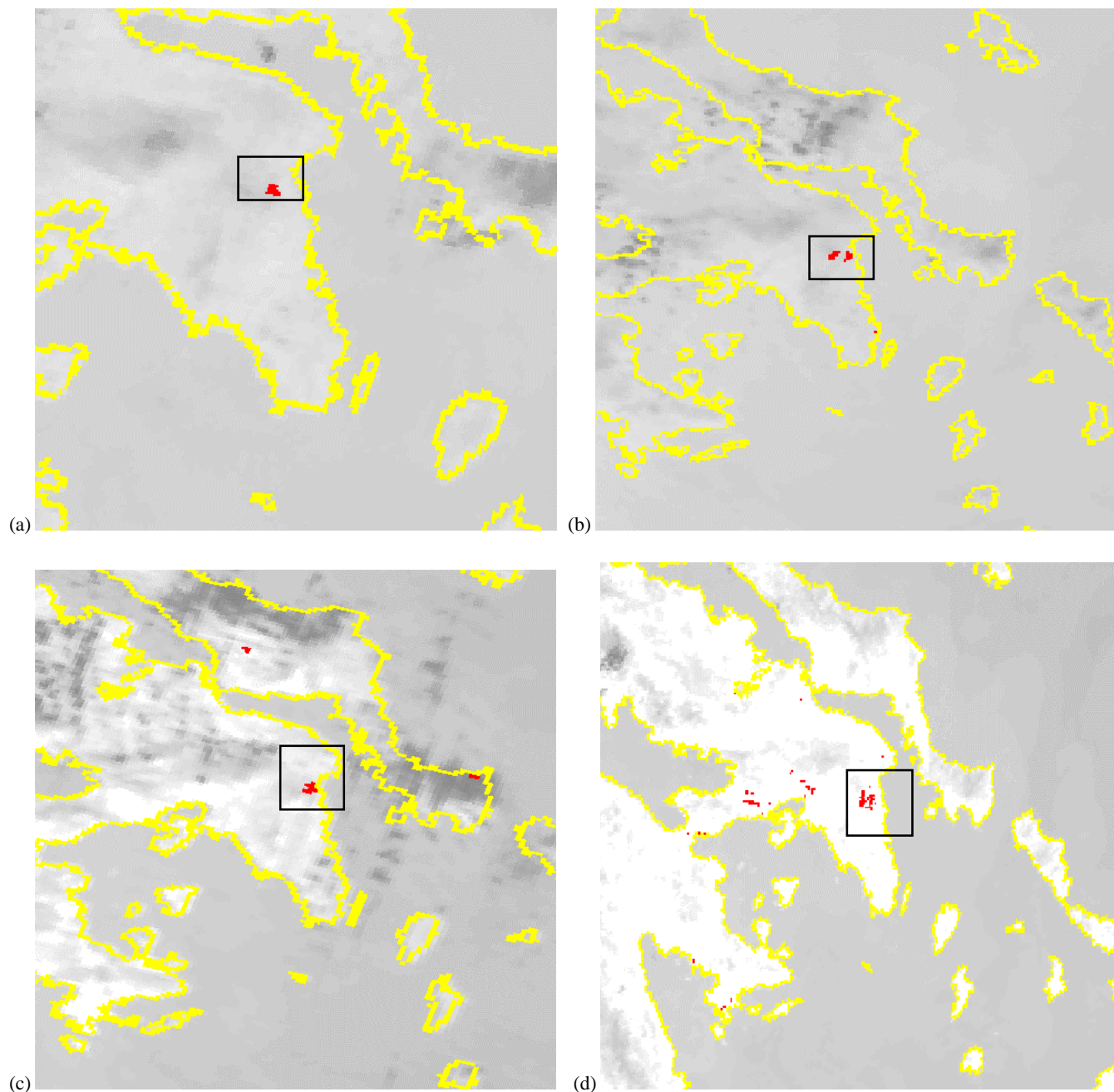


Fig. 6. (a) NOAA morning image of 21 July 1995 with surface temperature $>49^{\circ}\text{C}$. The burned area covers 6 km^2 . (b) NOAA night image of 21 July 1995 with surface temperature $>49^{\circ}\text{C}$. The burned area covers 22 km^2 . (c) NOAA image of 22 July 1995 with surface temperature $>49^{\circ}\text{C}$. The burned area covers 46 km^2 . (d) NOAA image of 25 July 1995 with surface temperature $>46^{\circ}\text{C}$. The burned area covers 63 km^2 . Series of NOAA images, processed to highlight the forest fire in Penteli, Attiki. The dark pixels within the rectangles show the area where the temperature is greater than the threshold of 49°C (for (a), (b) and (c)) and 46°C (for (d)).

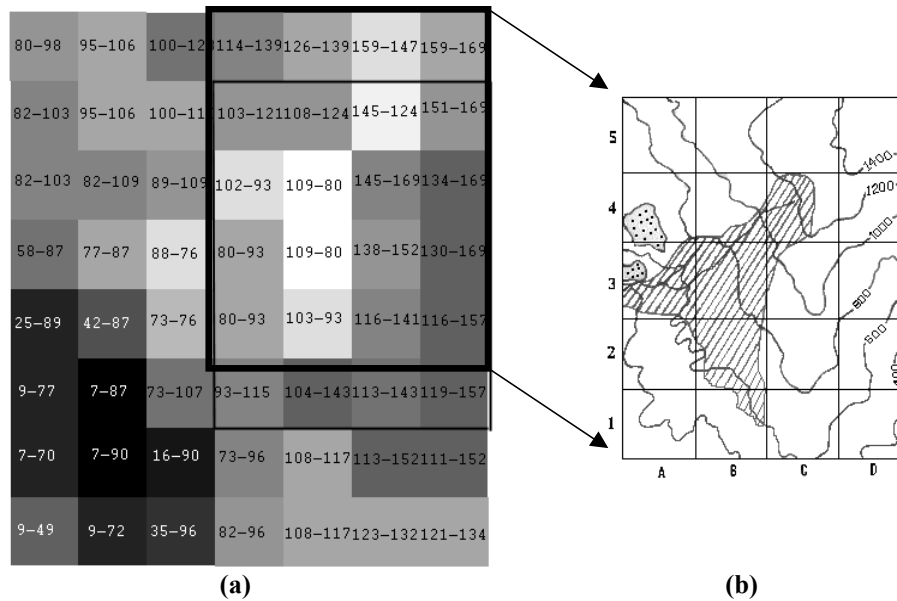


Fig. 7. Magnified window of NDVI differences image (a) showing the Katihori area. NDVI Pixel values before and after the fire are indicated. Dotted areas at A3 and A4 boxes (b) represent the villages Katihori and Portaria.

Table 5. Confusion matrix comparing the reference map with the extracted burned area from Landsat TM data

	Burned area	Non-burned area	number of pixels	% agreement
Estimated burned area	47392	1324	48716	97.28%
Estimated non-burned area	20715	111420	132135	84.32%
Total	68107	112744	180851	87.82%

September 1994. After the initiation of the forest fire in the morning of that day and until the sunset the fire spread was mainly restricted along the stream and the propagation direction was upslope (Fig. 7b). After the sunset as the mountain breeze was developing the fire intensified and spread across the stream outside the stream banks. During the fire evolution intensification occurred after the increase of wind speed and vice versa. In total, the fire burned more than 15 000 olive trees, about 0.02 km² of apple trees were ruined and a small number of animals was killed. Power supply network also suffered considerable damages. The total burned area was estimated by ground surveying from the Greek Forestry Department (personal communication) to 4.25 km².

Data from NOAA12 polar orbiting satellite were used for the calculation of NDVI for two days (14 and 23 September 1994) before and after the forest fire. The satellite trajectories for the two days differ by no more than 40 min°. A change detection technique, based on NDVI index derived from NOAA/AVHRR satellite data, is applied in the detection and monitoring of the burned area. Hence, a third image was produced by subtracting NDVI pixel values of the first image from the respective NDVI pixel values of the second image (e.g. 109–80 in the two most brighter pixels of Fig. 7a). A 7×8 pixel window of this image is pre-

sented in Fig. 7a in which NDVI differences are displayed in a 16 gray-scale palette. The sea water of the gulf generally showed pixel values of less than 90 in both cases (down left side). In the forest areas on mount Pelion values between 88 and 200 were observed. Within this scale negative differences (dark areas) represent NDVI increase and positive differences (light areas) NDVI decrease. Gray areas especially in the upper left represent densely forested areas with increasing tendency. Light areas in Fig. 7a are expected to represent fire-affected places.

The detected burned area consisted of five pixels, which indicated considerable differences in NDVI reduction. The examination of the actually burned area on Fig. 7b showed that only two pixels were completely affected by fire (B2, B3), in which NDVI reduction reached 29 (109–80). The initial values of 109 for these pixels were consistent with their coverage by olive fields and bushlands. The pixels A3, B1 and C4, also showed considerable (102–93, 103–93 and 145–124, respectively) decrease of the NDVI values although not completely covered. This was attributed to the domination of dense forest vegetation in the pixel area before the fire. It was assumed that the totally burned area corresponds to a NDVI change of 29 (= 109–80). Subsequently, the burned areas of the other three pixels were estimated proportionally

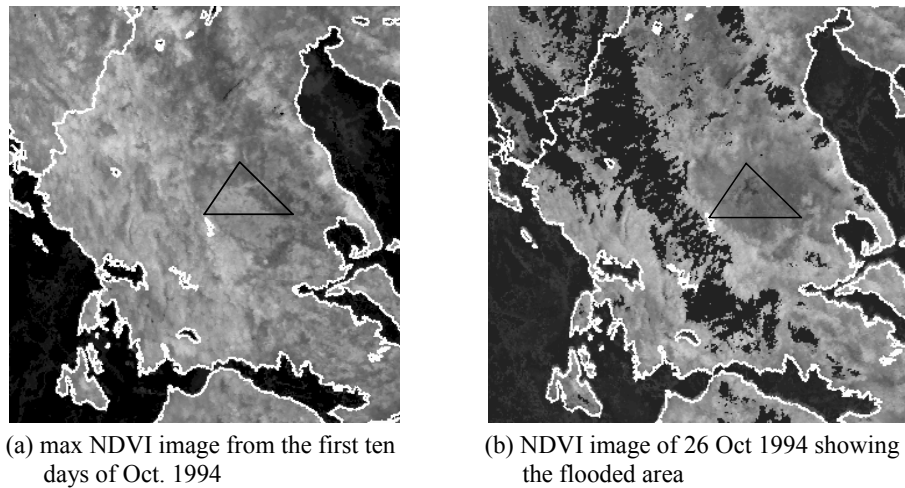


Fig. 8. Comparison between two NDVI images, before and after the flood in Thessaly, Greece. The first image shows the maximum NDVI image from the first ten days of October 1994, which will eventually be flooded. The flooded area can be seen, within the triangle, in the second image which is the NDVI image of 26 October 1994.

to their NDVI change. For example, in pixel A3 the change in NDVI value before and after the fire is $102 - 93 = 9$, and the burned area was estimated as $9/29 \times (1.1 \times 1.1) = 0.38 \text{ km}^2$. Similarly, the burned area in pixels B1 and C4 was estimated equal to 0.42 km^2 and 0.88 km^2 , respectively. The total burned area was estimated to about 4.1 km^2 , 2.42 km^2 for the two totally fire-affected pixels and 1.68 km^2 for the three partially fire-affected pixels. This figure of the totally burned area agrees well with the estimation made by the Greek Forestry Department (4.25 km^2).

Moreover, meteorological data were taken from three automatic stations namely, Volos, Velestino and Zagora in the vicinity of the fire. Using the meteorological data from these stations common indices were calculated for the assessment of the fire risk. The variation of temperature and relative humidity among the data from the three stations were not significant at the initiation of the forest fire (11:00 UT of 16 September 1994). However, the wind speed was quite different in the three stations. The wind speed in Volos was more favorable for fire initiation than in the other two stations.

The Angstrom's fire index for Volos, Velestino and Zagora meteorological stations was estimated to be 1.4, 1.5 and 2.3, respectively. Based on previous experience, the Angstrom index values suggest very favorable fire conditions for Volos and Velestino and favorable conditions for Zagora. Based on this method the estimated burned area, 3 km^2 , was considerably lower than the actually burned area.

The investigation of meteorological and satellite parameters during a forest fire in central Greece highlights the importance of local meteorological conditions in the fire risk assessment. Air temperature and relative humidity are important components of fire risk indices, but in order to improve performance wind speed and slope should be also incorporated. Positive indications were found for the detection and monitoring of burned area through NOAA satellites. NDVI

abrupt changes before and after the fire were observed for the burned areas. The magnitude of such changes depends on the amount of burned area per pixel, the vegetation density and the dominating species.

4.3 Flooding of central Thessaly, Central Greece (17–23 October 1994)

One case study dealing with the assessment of the flooded area is presented in this paper. The flood event of 17–23 October 1994 occurred in central Thessaly, Central Greece is analyzed herein. This flood event occurred in the central area of Thessaly (Fig. 1, area C). This particular area is located in the confluence of the seven major tributaries of Pinios River, namely, Enipeas River, Farsaliois River, Sofaditis River, Kalentis River, Pamisos River, Portaikos River and Lithaios River and suffers frequent and severe flooding, especially during widespread storm events. The tributaries drain the western and southern mountainous regions of Thessaly.

The storm of the study event started on 17 October and lasted till 23 October 1994 affecting most Greece. Quantitative assessment of the amount and intensity of the storm activity in the region of Thessaly was carried out by Dalezios et al. (1995). Hourly rainfall data were used in the analysis from ten automatic meteorological stations for the integration of daily rainfall depths during the period of the storm activity. The results have shown that very high rainfall depths have been observed in the eastern and the western parts of Thessaly, respectively, whereas in the central part the observed rainfall depths were normal. Moreover, time series of daily rainfall data from stations in the region were used for the development of the depth-duration-frequency relationships. This work showed that the 5-day storm corresponded to an average return period of five years, whereas for the west parts of Thessaly the 5-day storm corresponded to an average return period much higher than 100 years.

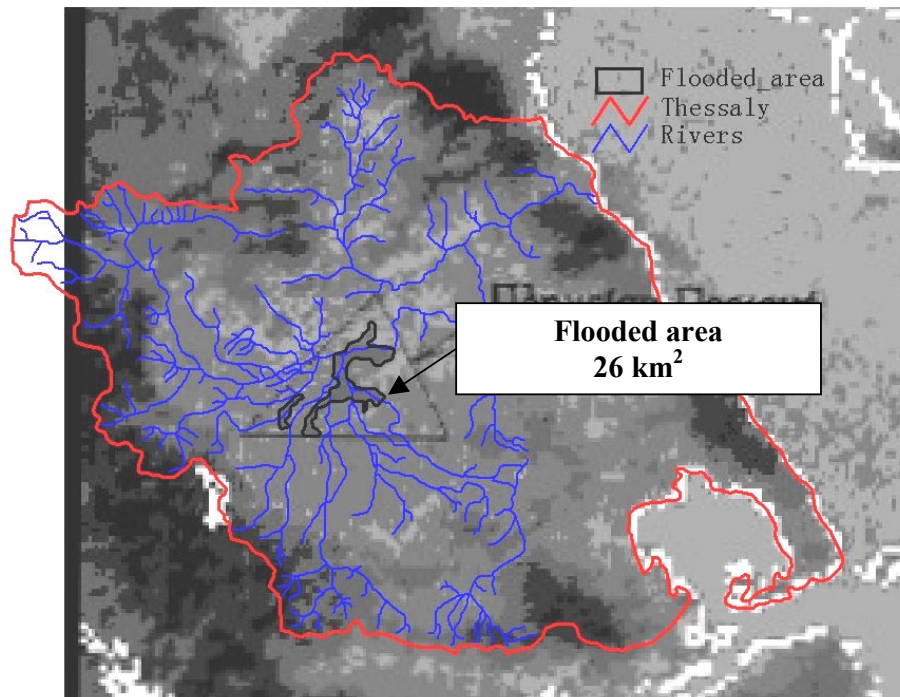


Fig. 9. Sea Surface Temperature image from the flooded area (26 October 1994) along with the rivers in Thessaly.

The assessment of the areal extent of the flooded area in the region of Thessaly has been accomplished by the use of NOAA/AVHRR NDVI. Firstly, daily NDVI image series was estimated for October 1994. Then, the Maximum Value Composites (MVC) images were produced from the maximum NDVI image series for the first ten days of October 1994. The advantage of using the MVC images is that the emissivity remains nearly constant within ten days, the cloud contamination effects are reduced and the effects caused by the angular viewing of the sensor are reduced (Dech et al., 1998). The MVC image of the first ten days of October 1994 is an indication of the green vegetation as it was before the storm. Figure 8a shows the MVC image for the first ten days of October 1994 in grayscale. The dark areas indicate low vegetation and as the pixel values become brighter, the vegetation increases. Figure 8b is the NDVI image of 26 October 1994, which was the first day after the storm with clear sky. Based on the same grayscale the flooded area can be delineated. The dark gray area within the triangular frame indicates the flooded area. The pixel values of the dark area have the lowest values of NDVI, which indicates the presence of water and the destruction of vegetation in the inundated area. The flooded area is estimated to be 26 km², which, agrees well with the ground surveying, and areal photographs estimation.

The flooded area was estimated by using the SST index. The SST was estimated as previously using Eq. (3). Furthermore, the SST was empirically determined with known water surfaces (e.g. sea). So, the low pixel values of the SST image, due to the presence of water, compared to the surrounding areas (mainly covered by vegetation) has been proven to

be a good indication of the flooded area. Figure 9 shows the Sea Surface Temperature (SST) image of 26 October 1994. This image was created from images taken the first day after the storm with clear sky (26 October 1994). This inundated area was estimated to be 26 km², which agrees almost perfectly to the estimated affected area by ground surveying and areal inspection and the NDVI results.

5 Conclusions

The increase in the natural disasters comes along with the rapid growth in the earth observation satellites. The range of new capabilities provided by the remotely sensed data can significantly contribute to early warning, monitoring and damage assessment and mitigation of affects of disasters.

In this work, the use of satellite remote sensing in the assessment and monitoring of forest fires and floods has been presented. The meteorological satellite system NOAA/AVHRR is explored towards meeting operational monitoring requirements. The emphasis has been placed on two hazards, namely forest fires and floods.

The analysis has indicated the growing potential and capabilities of using NDVI from NOAA/AVHRR into assessing and monitoring forest fires and floods. The SST has been also examined for the delineation of the areal extent of a flooded area and proved to be a powerful tool for operational damage assessment. In order to take advantage of these new technologies the capabilities of the satellite systems and techniques should be explored further. This is the only way to make these capabilities operationally useful and used.

Acknowledgements. The NOAA/AVHRR images were obtained from the NOAA/AVHRR receiving and processing system at the Laboratory of Agrometeorology, University of Thessaly covering the whole Greece. The Laboratory of Forest Management and Remote Sensing, Department of Forestry and Natural Environment, Aristotelian University of Thessaloniki provided the Landsat TM images.

References

- Barbosa, P. M., Grégoire, J.-M., and Pereira, J. M. C.: An algorithm for extracting burned areas from time series of AVHRR-GAC data applied at a continental scale, *Remote Sens. Environ.*, 69, 253–263, 1999.
- Bates, P. D., Horritt, M. S., Smith, C. N., and Mason, D.: Integrating remote sensing observations of flood hydrology and hydraulic modelling, *Hydrol. Process.*, 11, 1777–1795, 1997.
- Becker, F. and Li, Z. L.: Temperature independent spectral indices in thermal infrared band, *Remote Sens. Environ.*, 32, 17–33, 1990a.
- Becker, F. and Li, Z. L.: Towards a local split window method over land surface. *Int. J. Remote Sens.*, 3, 369–393, 1990b.
- Birkett, C. M.: Synergistic remote sensing of Lake Chad: Variability of basin inundation, *Remote Sens. Environ.*, 72, 218–236, 2000.
- B. U. R. L.: NOAA/AVHRR, Receiving and processing system, Report BURL V.3., Bradford University Research Ltd., UK, 1993.
- Chuvieco, E. and Martin, M. P.: A simple method for fire growth mapping using AVHRR channel 3 data, *Int. J. Remote Sens.*, 15, 3141–3146, 1994.
- Csiszár, I. and Kerényi, J.: The effect of the vegetation index on the daily variation of the active surface temperature, *Adv. Space Res.*, 16, 117–180, 1995.
- Dalezios, N. R.: Remote sensing of agricultural hazards, *Proceedings Space Congress, Bremen*, 23–25 May, 30–34, 1995.
- Dalezios, N. R., Tsidarakis, L. M., and Zarpas, C. D.: Quantitative characteristics of the flood of October 1994 in Thessaly, In: *Integrated Treatments for Flood Danger Reduction, Proceedings 2nd National Symposium, Athens*, 12–13 January, 183–191, 1995.
- Dalezios, N. R., Tzortzios, S., Domenikiotis, C., and Sarakatsanos, S.: The role of NDVI for the assessment of natural environmental hazards, In: *Computer technology in agricultural management and risk prevention, Proceedings 7th ICCTA-International Congress for Computer Technology in Agriculture, Florence, Italy*, 15–18 November, 383–390, 1995.
- Dech, S. W., Tungalagsaikhan, P., Preusser, C., and Meisner, R. E.: Operational value-adding to AVHRR data over Europe: methods, results, and prospects, *Aerosp. Science Techn.*, 5, 335–346, 1998.
- Domenikiotis, C., Dalezios, N. R., Loukas, A., and Karteris, M.: Agreement assessment of NOAA/AVHRR NDVI with Landsat TM NDVI for mapping burned forested areas, *Int. J. Remote Sens.* 23, 4235–4246, 2002.
- Eva, H. D. and Flasse, S.: Contextual and multiple-threshold algorithms for regional active fire detection with AVHRR data, *Remote Sens. Rev.*, 14, 333–351, 1996.
- Fernández, A., Illera, P., and Casanova, J. L.: Automatic mapping of surfaces affected by forest fires in Spain using AVHRR NDVI composite data, *Remote Sens. Environ.*, 60, 153–162, 1997.
- Foot, J. S.: Hazard warning in meteorology: the importance of remote sensing, In: *Proceedings of IDNDR Conference on Natural Hazards and Remote Sensing, London, UK*, 8–9 March 1994, 13–16, 1994.
- Flasse, S. and Ceccato, P.: A contextual algorithm for AVHRR fire detection, *Int. J. Remote Sens.*, 17, 419–424, 1996.
- Gupta, R. K., Prasad, S., and Viswanadham, T. S.: Estimation of surface temperature over agriculture region, *Adv. Space Res.*, 19, 3, 503–506, 1997.
- Hasegawa, I., Mitomi, Y., Nakayama, Y., and Takeuchi, S.: Land cover analysis using multi seasonal NOAA AVHRR mosaicked images for hydrological applications, *Adv. Space Res.*, 22, 677–680, 1998.
- Jayaraman, V., Chandrasekhar, M. G., and Rao, U. R.: Managing the natural disasters from space technology inputs, *Acta Astronautica*, 40, 291–325, 1997.
- Justice, C. O., Kendall, J. D., Dowty, P. R., and Scholes, R. J.: Satellite remote sensing of fires during the SAFARI campaign using NOAA advanced very high resolution radiometer data, *J. Geophys. Res.*, 101 (D19), 23 851–23 863, 1996.
- Kailidis, D. S.: *Forest fires, Giahoudi Giapouli Publications, Thessaloniki*, 1990.
- Kasischke, E. S. and French, N. H. F.: Locating and estimating the areal extent of wildland fires in Alaskan boreal forests using multiple-season AVHRR NDVI composite data, *Remote Sens. Environ.*, 51, 263–265, 1995.
- Kasischke, E. S., French, N. H. F., Harrell, P., Christensen, N. L., Ustin, S. L., and Barry, D.: Monitoring of wildfires in boreal forests using large area AVHRR NDVI composite image data, *Remote Sens. Environ.*, 45, 61–71, 1993.
- Kennedy, P. J., Belward, A. S., and Grégoire, J.-M.: An improved approach to fire monitoring in West Africa using AVHRR data, *Int. J. Remote Sens.*, 15, 2235–2255, 1994.
- Kerényi, J. and Putsay, M.: Investigation of Land Surface Temperature Algorithms Using NOAA/AVHRR Images, *Adv. Space Res.*, 26, 7, 1077–1080, 2000.
- Koutsias, N. and Karteris, M.: Logistic regression modelling of multitemporal Thematic Mapper data for burned area mapping, *Int. J. Remote Sens.*, 19, 3499–3514, 1998.
- Lyon, J. G., Yuan, D., Lunetta, R. S., and Elvidge, C. D.: A change detection experiment using vegetation indices, *Photogr. Engin. Remote Sens.*, 64, 143–150, 1998.
- Matson, M., Stephens, G., and Robinson, J. M.: Fire detection using data from NOAA-N satellites, *Int. J. Remote Sens.*, 8, 961–970, 1987.
- May, D. A., Stowe, L. L., Hawkins, J. D., and McClain, E. P.: A correction for Saharan dust effects on satellite sea surface temperature measurements, *J. Geophys. Res.*, 97 (C3), 3611–619, 1992.
- Pozo, D., Olmo, F. J., and Alados-Arboledas, L.: Fire detection and growth monitoring using a multitemporal technique on AVHRR mid-infrared and thermal channels, *Remote Sens. of Environ.*, 60, 111–120, 1997.
- Prata, A. J. and Platt, C. M. R.: Land surface temperature measurements from the AVHRR, In: *Proceedings of 5th AVHRR Data Users Conference*, 25–28 June, Tromsø, Norway, EUM P09, 433–438, 1991.
- Price, J. C.: Land surface temperature measurements from split window channels of the NOAA 7 advance very high resolution radiometer, *J. Geophys. Res.*, 89, 7231–7237, 1984.
- Pyne, S. J.: *Introduction to wildlife fire, Fire management in the United States*, John Wiley and Sons, New York, 1984.
- Rao, U. R.: *Space technology for sustainable development*, Tata McGraw-Hill, New Delhi, India, 1996.

- San Miguel-Ayaz, J., Vogt, J., De Roo, A., and Schmuck, G.: Natural hazards monitoring: Forest fires, droughts, and floods-The example of European pilot projects, *Surv. Geophys.*, 21, 291–305, 2000.
- Sheng, Y., Gong, P., and Xiao, Q.: Quantative dynamic flood monitoring with NOAA AVRR, *Int. J. Remote Sens.*, 22, 1709–1724, 2001.
- Sobrino, J. A. and Caselles, V.: A methodology for obtaining the crop temperature for NOAA-AVHRR data, *Int. J. Remote Sens.*, 12, 2461–2476, 1991.
- Sobrino, J. A., Caselles, V., and Coll, C.: Theoretical split window algorithms for determining the actual surface temperature, *Il Nuovo Cimento*, 16, 3, 219–236, 1993.
- Sobrino, J. A., Coll, C., and Caselles, V.: Atmospheric correction for land surface temperature using NOAA-11 AVHRR channels 4 and 5, *Remote Sens. Environ.*, 38, 19–34, 1991.
- Sobrino, J. A., Raissouni, N., and Li, Z. L.: A comparative study of land surface emissivity retrieval from NOAA Data, *Remote Sens. Environ.*, 75, 256–266, 2001.
- Spanos, S. I., Zarpas, C. D., and Dalezios, N. R.: Meteorological and satellite indices for the assessment of forest fires. In: *Proceedings of International Symposium on Applied Agrometeorology and Agroclimatology*, 24–26 April, Volos, Greece, 583–588, 1996.
- Townsend, P. A. and Walsh, S. J.: Modeling floodplain inundation using an integrated GIS with radar and optical remote sensing, *Geomorphology*, 21, 295–312, 1998.
- Williams, J.B.: Direct reception of satellite data for in-country warning, monitoring and mitigation of natural disasters in the developing world: the LARST approach. Hazard warning in meteorology: the importance of remote sensing. In: *Proceedings of IDNDR conference on Natural Hazards and Remote Sensing*, London, UK, 8–9 March 1994, 22–25, 1994.
- Ulivieri, C. and Cannizzaro, G.: Land surface temperature retrievals from satellite measurements, *Acta Astronautica*, 12, 997–985, 1985.
- Ulivieri, C., Castronuovo, M. M., Francioni, R., and Cardillo, A.: A split window algorithm for estimating land surface temperature from satellites, *Adv. Space Res.*, 14, 3, 59–65, 1994.
- Van De Gried, A. A. and Owe, M.: On the relationship between thermal emissivity and the normalized difference vegetation index for natural surfaces, In: *J. Remote Sens.*, 14, 1119–1137, 1993.
- Zhou, G., Luo, J., Yang, C., Li, B., and Wang, S.: Flood monitoring using multi-temporal AVHRR and RADARSAT imagery, *Photogr. Engin. Remote Sens.*, 66, 633–638, 2000.